Journal of the Meteorological Society of Japan, Vol. 75, No. 3, pp. 641–656, 1997

Propagation of Waves Exited by Localized Episodic Heating in the Tropics and Their Effect on the Middle Atmosphere: Comparison between two QBO Phases

By Takeshi Horinouchi and Shigeo Yoden

Department of Geophysics, Kyoto University, Kyoto 606-01, Japan

(Manuscript received 1 June 1996, in revised form 13 February 1997)

Abstract

Propagation of waves excited by localized episodic heating in the tropical troposphere and their effect on the middle atmosphere are investigated numerically with a global primitive-equation model in which a realistic radiation scheme for the middle atmosphere is incorporated. Equinoctial initial states with two opposite phases of the quasi-biennial oscillation (QBO) are used for comparison of the propagation and the effect of the waves.

Time evolutions of the responses of the equinoctial initial states are not much different from the linear responses of a resting atmosphere obtained by Horinouchi and Yoden (1996). If the duration of the heating is small (less than about a day), Eliassen-Palm (EP) flux in the middle atmosphere is mainly due to gravity waves including Kelvin waves, while if the duration is large (more than about a day), it is mainly due to Kelvin waves, Rossby waves, and Rossby-gravity waves.

In the westerly-shear phase of the QBO, westerly acceleration comparable to or a little smaller than that required by the QBO is obtained for wide range of heating parameters, while in the easterly-shear phase, realistic easterly acceleration cannot be obtained if the heating events have large time and horizontal scales (more than about a day and a few thousand kilometers). Gravity waves propagating into the low- and mid-latitude mesosphere are affected by the QBO. The difference in the divergence of the EP flux due to gravity waves may explain the observed quasi-biennial variations in the low- and mid-latitude mesosphere.

Excitation of the global normal mode 5-day wave is sensitive to the QBO phase. Since such a QBO modulation has not been observed, this result implies that the source of the 5-day wave in the real atmosphere is not or not only in the tropics, but a considerable portion of the wave is excited outside the tropics.

1. Introduction

Various kinds of vertically propagating wave motion have been observed in the equatorial middle atmosphere. The primary source of these equatorial waves has been considered to be in cumulus convective systems in the tropical troposphere. In order to understand the excitation of these waves, some authors have theoretically studied the atmospheric responses to localized transient heating in the tropical troposphere (Holton, 1972; Hayashi, 1976; Itoh 1977; Salby and Garcia, 1987; Garcia and Salby, 1987; Manzini and Hamilton, 1993; Bergman and Salby, 1994; Horinouchi and Yoden, 1996). In these studies the heating is prescribed externally as a large-scale heating in organized cumulus convective systems. This is the simplest way to investigate the large-scale wave excitation by cumulus convections.

Among them Salby and Garcia (1987) studied linear responses of a resting spherical atmosphere to localized episodic heating in a stochastic flame work. They showed that the dominant responses are not only the vertically-propagating, equatorially-trapped waves but also global normal modes. A detailed historical review of the studies of the middle-atmospheric responses to transient heating in the tropical troposphere is given by Horinouchi and Yoden (1996, hereafter referred to as HY).

HY extended the study by Salby and Garcia (1987) by using the method of separation of variables, which enabled the investigation of energy and momentum distribution to various kinds of wave. They also classified characteristic patterns of the time evolutions of the responses depending on the time and horizontal scales of the heating.

HY used a resting basic state and a constant coefficient of the Newtonian cooling, which was the only dissipative term in their study. Although the response near the heating region is well described under these assumptions, the wave propagation far from the forcing region is largely affected by the basic state (*i.e.* meridional and vertical distributions of zonally averaged wind and temperature) and damping processes in the real atmosphere. Thus, in this paper, we investigate wave propagation in realistic basic states using an accurate radiation scheme. We also estimate the effect of the vertically propagating waves on the middle atmosphere by using the Eliassen-Palm (EP) flux diagnoses.

As for the excitation of global normal modes, Manzini and Hamilton (1993) showed that convective heating was not important for the excitation in a simulation with a general circulation model (GCM). On the other hand, HY estimated that stochastic random heating processes with a realistic total amount of heating would excite a realistic amplitude of the "5-day wave" if the heating had some appropriate spectra. The excitation of the normal modes by heating in the tropics is the other subject investigated in this study.

Section 2 describes the numerical models and experimental parameters. Sections 3–5 describe the results; Section 3 shows time evolutions of the responses, Section 4 describes the time-averaged EP flux and its statistical interpretations, and Section 5 describes the global normal modes. Discussion is given in Section 6, and conclusions are given in Section 7.

2. Models and experiments

2.1 Primitive-equation model with a log-pressure vertical coordinate

We used a full nonlinear primitive-equation model with a log-pressure vertical coordinate in the global spherical domain. This is a spectral model with a triangular truncation of T42 or T21, and the vertical resolution is about 1.5 km. The model is based on a simple GCM (AGCM5) in GFD-DENNOU Library.

An accurate radiation scheme developed by Zhu (1994) for the middle atmosphere is incorporated into the model. Both of the short-wave and long-wave calculations are based on the k-distribution method. Absorption constituents are H_2O, CO_2 and O_3, whose mixing ratios are assumed to be horizontally uniform with the vertical profiles listed in U.S. Standard Atmosphere (1976).

The model has horizontal viscosity terms proportional to ∇^8 with a 3-hour e-folding time for the maximum total wavenumber and the vertical eddy diffusion closure proposed by Mellor and Yamada (1974, the level 2 closure) with the minimum value of 0.1 m^2s^{-1} for the diffusion coefficients.

The bottom boundary is at $\zeta = 2$ ($p \sim 140$ hPa; $\zeta \equiv -\log(p/p_s)$ where $p_s \equiv 1000$ hPa). We do not force the heating explicitly in the troposphere, but specify the linear response of a resting atmosphere to the heating at the bottom boundary. The linear response is calculated separately by the same method as in HY (see their sections 2 and *4.1*) except for the Newtonian cooling rate of 1/15 day^{-1}.

Since the linear response is obtained as a summation of Hough functions, we can choose any arbitrary components (for example, Rossby waves) for the bottom forcing in the nonlinear model. Such separation enables the analysis of the propagation of the components. This is the reason why such an indirect method is used instead of forcing the heating directly in a model with the troposphere.

The top boundary is at ζ=12. To suppress the spurious reflection at the top boundary, Rayleigh friction is incorporated near the top; the coefficient is

$$\alpha_R = 1 \times 10^{1.4\tanh[(\zeta-9.7)/3.3-0.4]} \ \mathrm{day}^{-1}, \quad (1)$$

which is equal to 2.8 day^{-1} at ζ=12, 0.53 day^{-1} at ζ=10, and 0.086 day^{-1} at ζ=8.

2.2 Primitive-equation model with a σ vertical coordinate

A supplemental primitive-equation model with a σ vertical coordinate ($\sigma = p/p_{\mathrm{surface}}$) is used in Section 5 to study the global normal modes. The free-slip condition is applied at the surface without topography. As the forcing, diabatic heating is specified explicitly in the troposphere as in HY. Radiative processes are substituted by Newtonian cooling of a constant rate 1/15 day^{-1}. Other parts are identical to the log-pressure model described above.

2.3 Basic (initial) states

An initial state for the log-pressure model is a steady states obtained in the zonally symmetric version of the model.

Equinoctial solar insolation is assumed in the radiation calculation to obtain an equinoctial initial state. Wind velocity at the bottom boundary ($\zeta = 2$) is assumed to be zero, and wind velocity near the mesopause is kept to about zero by the Rayleigh friction near the top boundary.

Two opposite zonal forcing of the QBO phases are superposed on the radiative forcing by incorporating Rayleigh friction only in the zonal mean zonal wind in the equatorial lower stratosphere. The zonal wind is relaxed to the following prescribed state:

$$U_{\mathrm{QBO}} \equiv 45 \times \cos\left(2\pi\frac{\zeta - 3.5}{6} + \theta_{\mathrm{QBO}}\right) \times \exp\left[-\left(\frac{\varphi}{\Phi_{\mathrm{QBO}}}\right)^2\right]$$

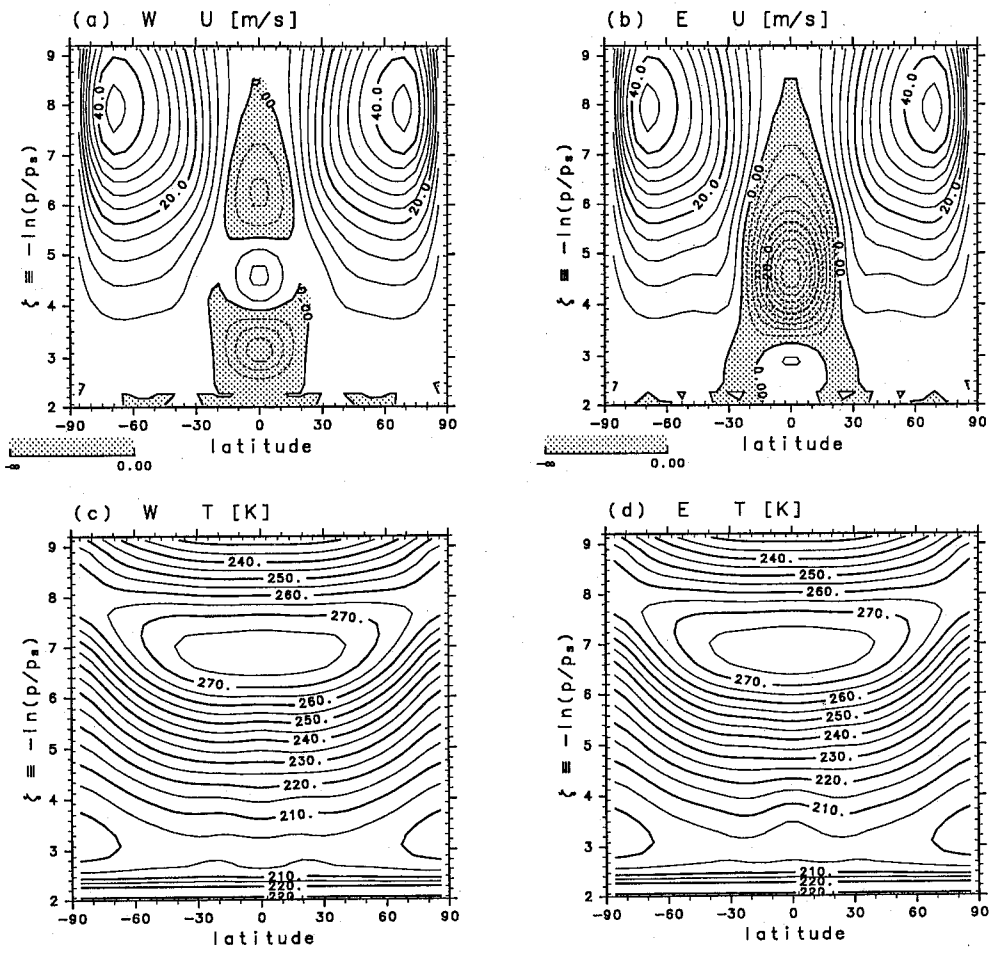

Fig. 1. Zonal wind and temperature of the equinoctial basic states with two opposite phases of the QBO; W (westerly shear) and E (easterly shear). Note that the sponge layer where Rayleigh friction is incorporated near the top boundary is excluded in these panels. Contour intervals: (a),(b) 4 ms^{-1}; (c),(d) 5 K.

$$\times \begin{cases} \exp\left[-\left(\frac{\zeta-3.2}{0.68}\right)^2\right], & \text{for } \zeta < 3.2, \\ 1, & \text{for } 3.2 < \zeta < 4.1, \\ \exp\left[-\left(\frac{\zeta-4.1}{1.37}\right)^2\right], & \text{for } \zeta > 4.1, \end{cases} \quad [\mathrm{ms}^{-1}] \quad (2)$$

where two particular phases of the QBO are adopted with $\theta_{\mathrm{QBO}} = -\pi/2$ for the "westerly shear" phase and $\theta_{\mathrm{QBO}} = \pi/2$ for the "easterly shear" phase. Latitudinal width is set to be $\Phi_{\mathrm{QBO}} = 17°$. The [relaxation time]$^{-1}$ is

$$\alpha_{R,\mathrm{QBO}} = \frac{1}{30} \times \exp\left[-\left(\frac{\varphi}{\Phi_{\mathrm{QBO}}}\right)^2\right] \times \begin{cases} \exp\left[-\left(\frac{\zeta-3.2}{0.68}\right)^2\right], & \text{for } \zeta < 3.2, \\ 1, & \text{for } 3.2 < \zeta < 4.1, \\ \exp\left[-\left(\frac{\zeta-4.1}{1.37}\right)^2\right], & \text{for } \zeta > 4.1. \end{cases} \quad [\mathrm{day}^{-1}] \quad (3)$$

The obtained steady states are shown in Fig. 1; one state for $\theta_{\mathrm{QBO}} = -\pi/2$ is referred to as "W" (westerly shear), and the other for $\theta_{\mathrm{QBO}} = \pi/2$ is referred to as "E" (easterly shear). Here westerly shear means positive vertical shear ($dU/dz > 0$) around $\zeta = 3.5$. Equation (2) is similar to that used by Garcia and Salby (1987) to represent the zonal wind of the QBO superposed on a climatological basic state. The values of the coefficients in their equation such as the amplitude are modified empirically to derive appropriate basic states. However, there remains an error that the zonal wind in the QBO region tends to be more easterly than in the real atmosphere; the maximum westerly wind speed in "W" is 9 ms^{-1} and the maximum easterly wind speed is 38 ms^{-1}. The former value is smaller than that in the real atmosphere (20 ms^{-1}) while the latter is comparable to or slightly larger than that (35 ms^{-1}).

Another initial state is obtained in an artificial

(a)

	Basic state	Scale of the heating	φ_0	Numerical resolution
(W-s-0)	W	small	0°	T42
(W-s-10)	W	small	10°	T42
(W-l-0)	W	large	0°	T21
(W-l-10)	W	large	10°	T21
(E-s-0)	E	small	0°	T42
(E-s-10)	E	small	10°	T42
(E-l-0)	E	large	0°	T21
(E-l-10)	E	large	10°	T21
(R-s-0)	R	small	0°	T21
(R-s-10)	R	small	10°	T21
(R-l-0)	R	large	0°	T21
(R-l-10)	R	large	10°	T21

(b)

$(X)_g$, X=W-s-0,W-s-10,..	Same as (X) but for forcing the"gravity wave" components	T21
$(X)_R$, X=W-s-0,W-s-10,..	Same as (X) but for forcing the "Rossby wave" components	T21

Table 1. Summary of experiments.

framework with a uniform solar insolation in all latitudes. The resultant steady state is at rest, and is referred to as "R".

Since the response in each experiment is not large enough to alter these initial states substantially, the initial states can be regarded as the basic states for the experiments.

2.4 Localized episodic heating

The localized episodic heating in the tropical troposphere is assumed to have the following form as in Salby and Garcia (1987), Garcia and Salby (1987), and HY:

$$J = J_0\, j(\zeta) \times \exp\left[-\frac{(\lambda-\lambda_0)^2}{2\Lambda^2} - \frac{(\varphi-\varphi_0)^2}{2\Phi^2} - \frac{(t-t_0)^2}{2T^2}\right], \tag{4}$$

where J_0 is a constant, and the vertical structure of the heating is given by

$$j(\zeta) = \begin{cases} \sin(\pi\zeta/1.5), & \text{for } 0 < \zeta \le 1.5, \\ 0, & \text{for } \zeta > 1.5. \end{cases} \tag{5}$$

Since the spherical geometry is symmetric about zonal direction, λ_0 is fixed to 180°, and t_0 is also fixed to 0. The meridional center of heating φ_0 is set equal to 0° or 10°, and the scales (Λ, Φ, T) are set equal to (3°, 3°, 0.1 days) or (10°, 10°, 0.5 days); the former combination is referred to as "small"-scale, or "s", and the latter as "large"-scale, or "l" in the following. These values are identical to those used in HY. The maximum value of the heating rate J_0 is set equal to 20 Kday^{-1}, which is a typical value of the heating observed in a cloud cluster(*e.g.* Johnson, 1992). Choice of these parameters in each experiment is summarized in Table 1a.

As mentioned in Subsection *2.1*, the linear response to the heating described above is used as the bottom boundary forcing in the log-pressure model at $\zeta = 2$. In addition to the standard experiments in which the whole linear response is forced, some experiments are also done in which only the "gravity wave" components (inertio-gravity waves, Kelvin waves, and eastward Rossby-gravity waves) or the "Rossby wave" components (Rossby wave and westward Rossby-gravity waves) of the linear response are forced. These experiments are referred to as abbreviations with suffix "g" or "R" (Table 1b). Note that the whole forcing is the summation of the forcing of the "gravity wave" and "Rossby wave" components. The "l" experiments are done with T21 truncation, and the standard "s" ones basically with T42. Other "s" experiments, however, are done with T21. The "s" experiments are integrated from $t = -1$ day while the "l" ones from $t = -3$ days, and the integration period is 30 days for all experiments.

Detailed analyses of the results of the time integrations show that $(X) \simeq (X)_g + (X)_R$, that is, the interaction between "gravity waves" and "Rossby waves" is weak in each standard experiment. (For this comparison, the standard "s" experiments were also done with T21 truncation.)

2.5 Responses to stochastic random heating processes

Although only one heating event is forced in each experiment, it is possible to estimate time-averaged

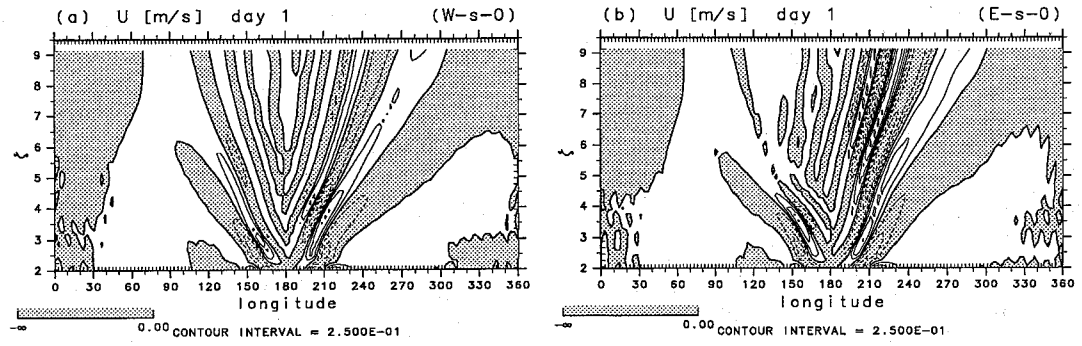

Fig. 2. Longitude-height sections of the zonal wind deviation from the zonal mean u' on the equator at $t = 1$ day for the experiments (W-s-0) and (E-s-0). Negative values are shaded.

properties of the response to a stochastic random heating process in which the same Gaussian heating events occur randomly with longitude and time without mutual correlation. The estimation method that was described and used in HY is also used in this study (Subsection *4.2*). We assume that the total heating averaged per day in the stochastic heating process is identical with the climatological latent heat release in the equatorial region between $\varphi = \pm 15°$. If we further assume that the responses to every heating events in the stochastic process do not interact with each other, we can estimate time-averaged properties of the response to such a process only by multiplying those of the response to one event of the Gaussian heating by a constant factor.

3. Time evolutions

3.1 Responses to "small"-scale heating

Simulated nonlinear responses of the resting atmosphere R to the "s" heating are similar to the linear responses described in HY (see their Figs. 6–8). Horizontal wind fields show that gravity wave response expands concentrically at the beginning until about $t = 1$ day, and then the response spreads zonally in low latitudes. In the experiments with the equinoctial basic states (W and E), horizontal wind fields evolve in the similar way. Above the QBO region in the experiments with E, however, the concentric pattern at the beginning is not symmetric because of the strong easterly wind of the QBO; magnitude in the west of the heating is weaker than that in the east. Figure 2 shows equatorial cross sections of the zonal wind deviation from the zonal mean (u') at $t = 1$ day for the experiments (W-s-0) and (E-s-0). Above the QBO region the latter has more eastward-westward asymmetry with respect to λ_0 ($= 180°$) than the former.

Figure 3 shows time-longitude sections of equatorial u' at $\zeta = 3.9$ ($p \sim 20$ hPa; left panels) and $\zeta = 7$ ($p \sim 1$ hPa; right panels) for the experiments (W-s-0) and (E-s-0). Above the QBO region (right panels), eastward-moving waves (waves with eastward phase velocities) in E are much larger than those in W, while westward-moving waves are larger in W. On the other hand, this relationship is reversed in the QBO region (left panels): eastward- (westward-) moving waves in W are larger (smaller) than those in E. Both relationships are explained by the WKB theory as in the following manner. Above the QBO region, the amplitude of the eastward-moving waves in E is larger than that in W since the eastward-moving waves do not suffer much attenuation during the propagation in the easterly wind of the QBO region because of the larger group velocities related to the larger intrinsic phase speeds. In the QBO region, on the other hand, the amplitude of the horizontal wind due to eastward-moving waves is smaller than that in W because of the larger intrinsic phase speeds (Lindzen, 1971); the vertical wavelength of waves in E is elongated so that the horizontal wind amplitude is reduced.

Gravity waves in the "s" experiments propagate into mid and high latitudes; the concentric gravity-wave responses are wider for larger altitudes. Figure 4 shows time-latitude sections of meridional wind deviation from the zonal mean (v') at $\lambda = 180°$ for Experiment (W-s-0). At $\zeta = 3.5$ (a), the initial concentric response spreads into mid-latitudes of $|\varphi| \lesssim 40°$ by $t = 2$ days, and then it spreads zonally within $\varphi = \pm 30°$ (not shown). At $\zeta = 7$ (b), the response spreads into high latitudes of $|\varphi| \lesssim 70°$ by $t = 3$ days. Afterwards, it also spreads zonally; the eastward-moving waves are confined within a low-latitude band of $|\varphi| \lesssim 30°$ while the westward-moving waves are confined within $|\varphi| \lesssim 45°$. This difference is explained in terms of the critical latitudes for the gravity waves; because of the equinoctial mid-latitude westerly wind, the critical latitude where the intrinsic angular frequency of a wave coincides with the local Coriolis parameter is higher in general for a westward-moving gravity wave than that for an eastward-moving one. This difference

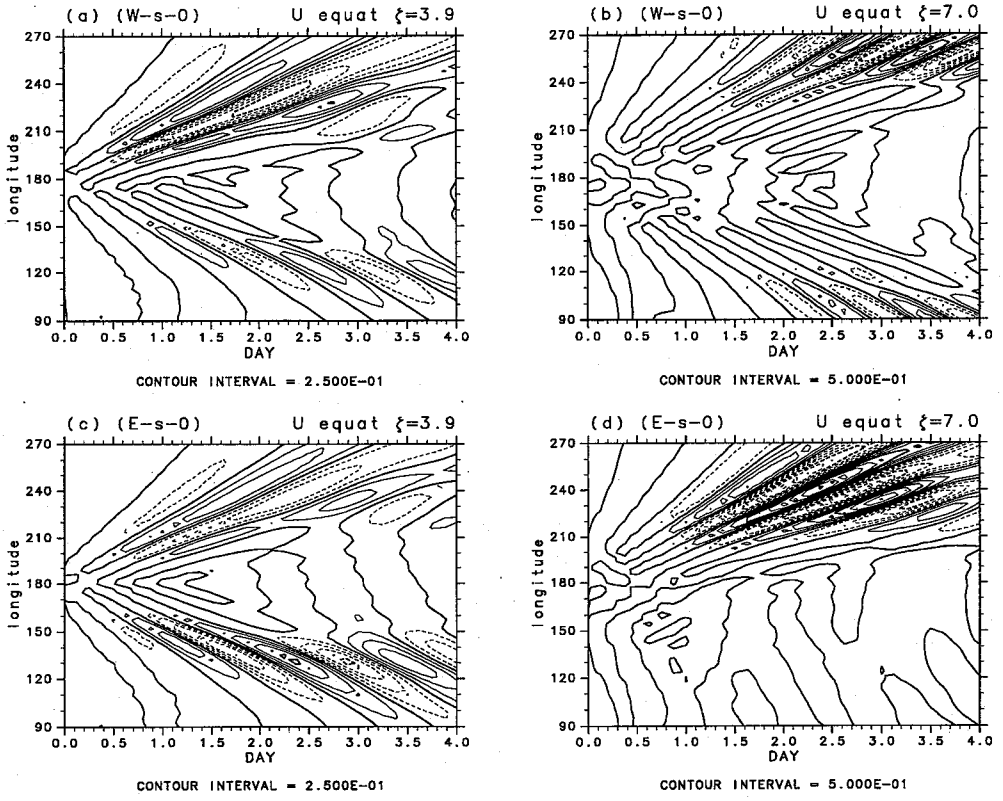

Fig. 3. Time-longitude sections of u' on the equator at $\zeta = 3.9$ ($p \sim 20$ hPa) and $\zeta = 7 (p \sim 1$ hPa) for the experiments (W-s-0) and (E-s-0).

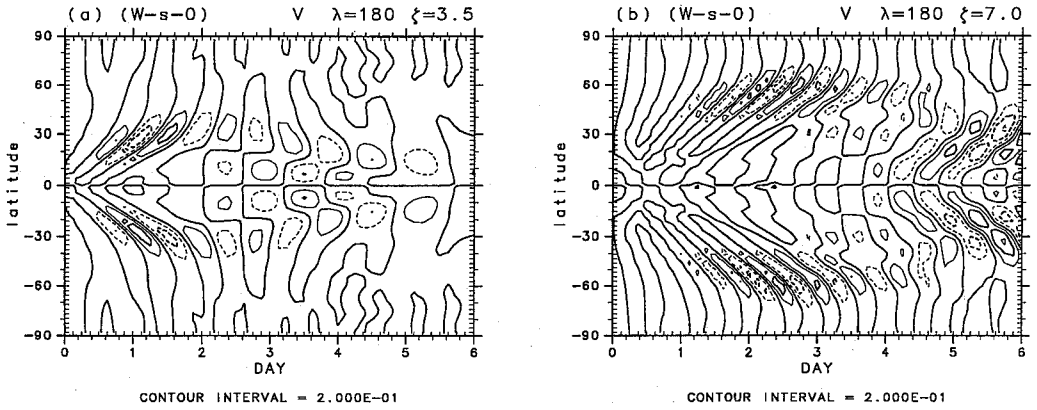

Fig. 4. Time-latitude sections of meridional wind deviation from the zonal mean v' at $\lambda = 180°$ for Experiment (W-s-0).

is also observed in the experiments with E. Moreover, the westward-moving waves in E propagate into higher latitudes than those in W as seen in Subsection *4.1*.

We have described the responses to the heating events with $\varphi_0 = 0°$. Similar results are also obtained in the experiments with $\varphi_0 = 10°$.

3.2 Responses to "large"-scale heating

As in the linear study by HY, the responses of the resting basic state to the "I" heating show "Gill pattern" (Gill, 1980) at the beginning in the lower stratosphere; Kelvin waves appear in the east of the heating region while Rossby waves appear in the west. In the experiment with $\varphi_0 = 10°$ (R-l-10), Rossby-gravity waves also appear in the east of the heating region. Then the response spreads zonally

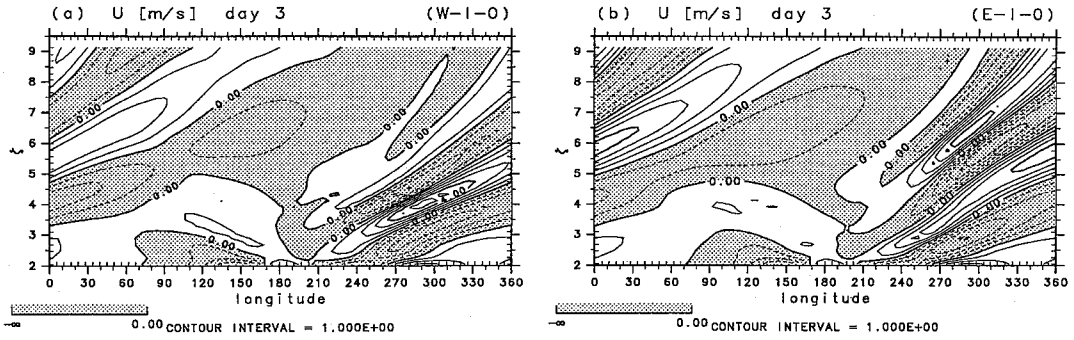

Fig. 5. As in Fig. 2, but for the experiments (W-l-0) and (E-l-0) at $t = 3$ days.

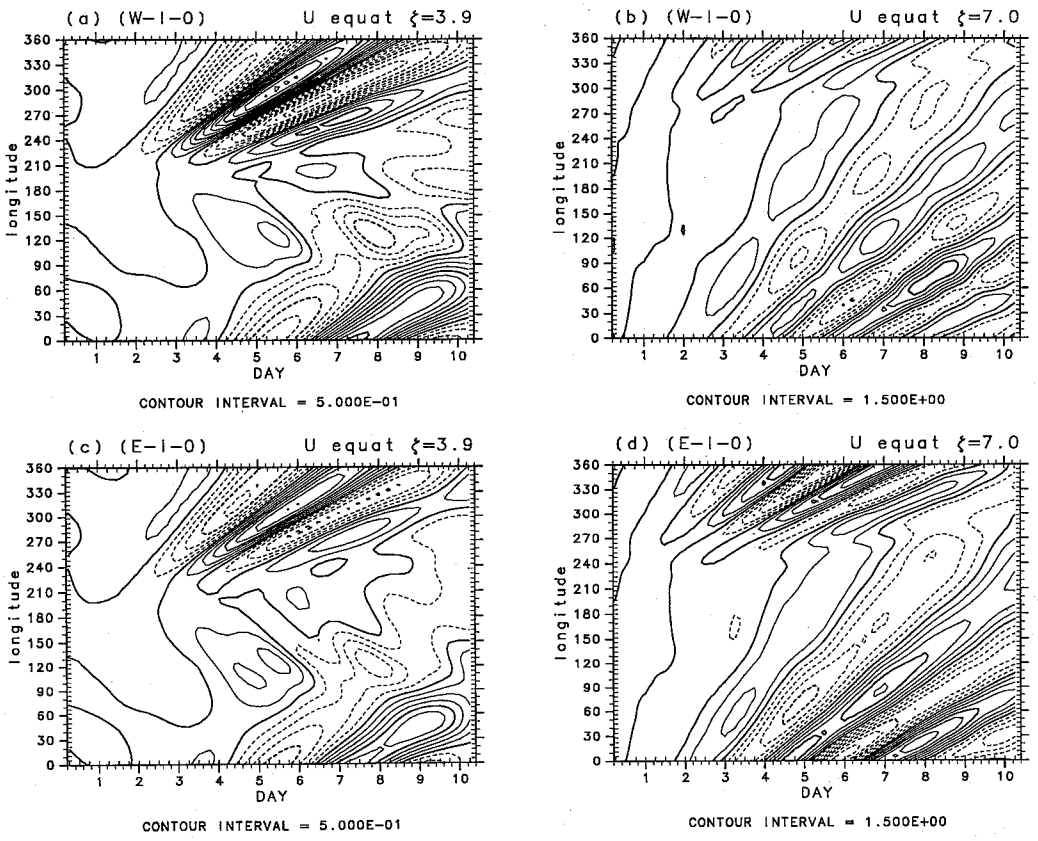

Fig. 6. As in Fig. 3, but for the experiments (W-l-0) and (E-l-0).

in low latitudes afterwards. Dominant responses are Kevin waves of zonal wavenumber $s = 1$-3.

In the experiments with the equinoctial basic states, horizontal wind fields show similar time evolutions to those of the resting basic state. Figure 5 shows equatorial cross sections of u' at $t = 3$ days for the "l" experiments of $\varphi_0 = 0°$. In both cases of (W-l-0) and (E-l-0), Kelvin waves are emitted in the east of the heating region and spread into the middle atmosphere; they gradually spread over the whole equatorial middle atmosphere with time. On the other hand, Rossby waves are emitted in the west of the heating and are confined near the heating region.

Figure 6 shows time-longitude sections of u' for experiments (W-l-0) and (E-l-0). Amplitude of Kelvin waves in the middle atmosphere is affected by the QBO phases, and the difference between W and E is in the same way as in the "s" experiments (Fig. 3).

Experiments with the "l" heating with $\varphi_0 = 10°$ show similar time evolutions of flow fields, although Rossby-gravity waves are dominant next to the Kelvin waves.

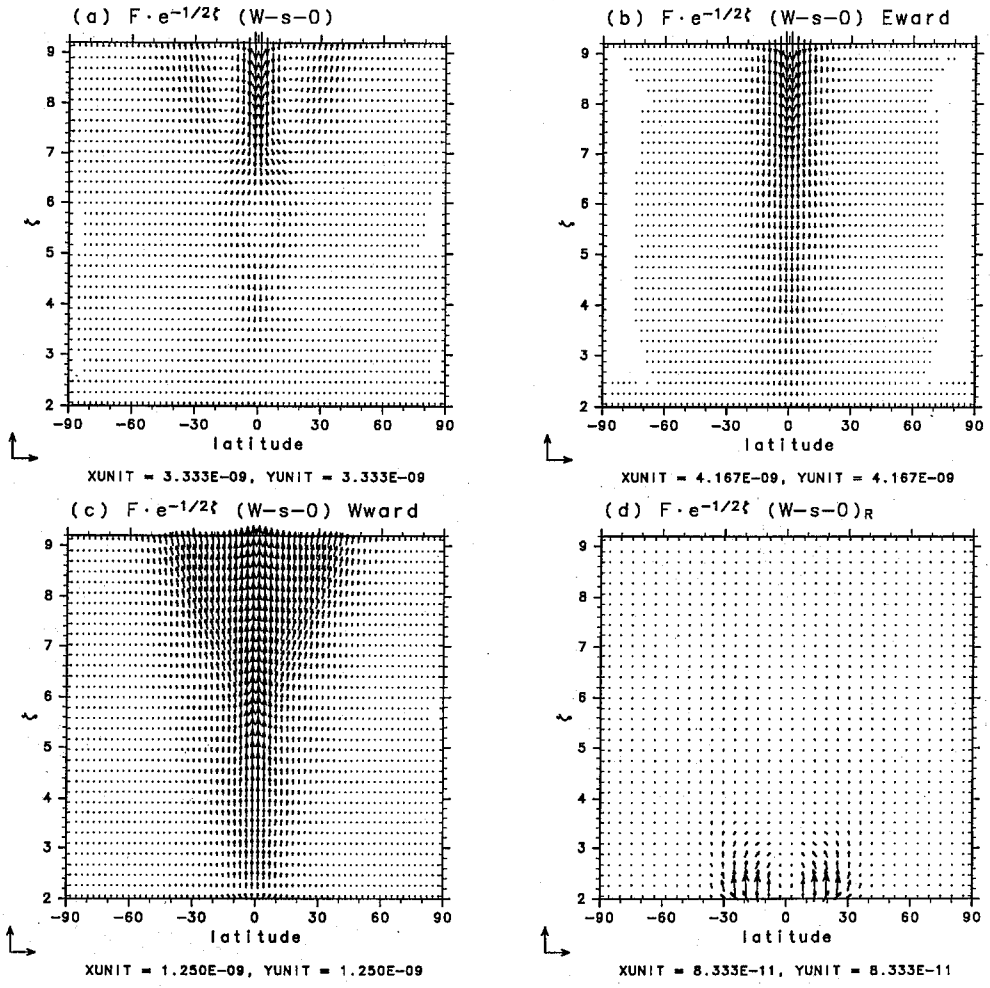

Fig. 7. Time-averaged EP flux for Experiment (W-s-0): (a) all components, (b) eastward-moving components, and (c) westward-moving components. Time-averaged EP flux for Experiment $(\text{W-s-0})_R$ is in (d). The flux is multiplied by $\exp(-\zeta/2)$ for graphical convenience and its meridional component is multiplied by a constant so that the directions of arrows represent those of the wave propagation correctly in each panel. The scale of arrows is indicated below each panel.

4. Eliassen-Palm (EP) flux

4.1 Time averaged EP flux

Figure 7a shows the time average of the EP flux for the integration period (30 days) obtained in Experiment (W-s-0). It is multiplied by $\exp(-\zeta/2)$ for graphical convenience and the meridional component is multiplied by a factor so that arrows indicate the direction correctly in the panel. The EP flux is divided into the contributions of eastward- (b) and westward- (c) moving components using two-dimensional (time and longitude) Fourier transform. Figure 7d also shows the time averaged EP flux for Experiment $(\text{W-s-0})_R$, in which only "Rossby wave" components are forced. Note that the scales of arrows in the four panels are different. The contribution of "Rossby waves" to EP flux is very weak. Thus the EP flux shown in a–c is mainly due to "gravity waves". Below $\zeta = 6$, both of the eastward- and westward-moving components are confined near the equator. Above $\zeta = 6$, the westward-moving component spreads meridionally, while the eastward-moving component is confined near the equator because the critical latitude is different between the westward- and eastward-moving waves due to the equinoctial mid-latitude westerly wind as mentioned in Subsection *3.1*. The westward-moving gravity waves carry westward momentum into the mid-latitude mesosphere.

Figure 8 shows the time-averaged EP flux for Experiment (E-s-0). The contribution of "Rossby waves" is very weak as in (W-s-0), and that of eastward-moving "gravity waves" is dominant. The eastward-moving component is confined near the equator for all altitudes, while the westward-moving component is divided around ζ = 4-5 and propagates into northern and southern mid-latitudes.

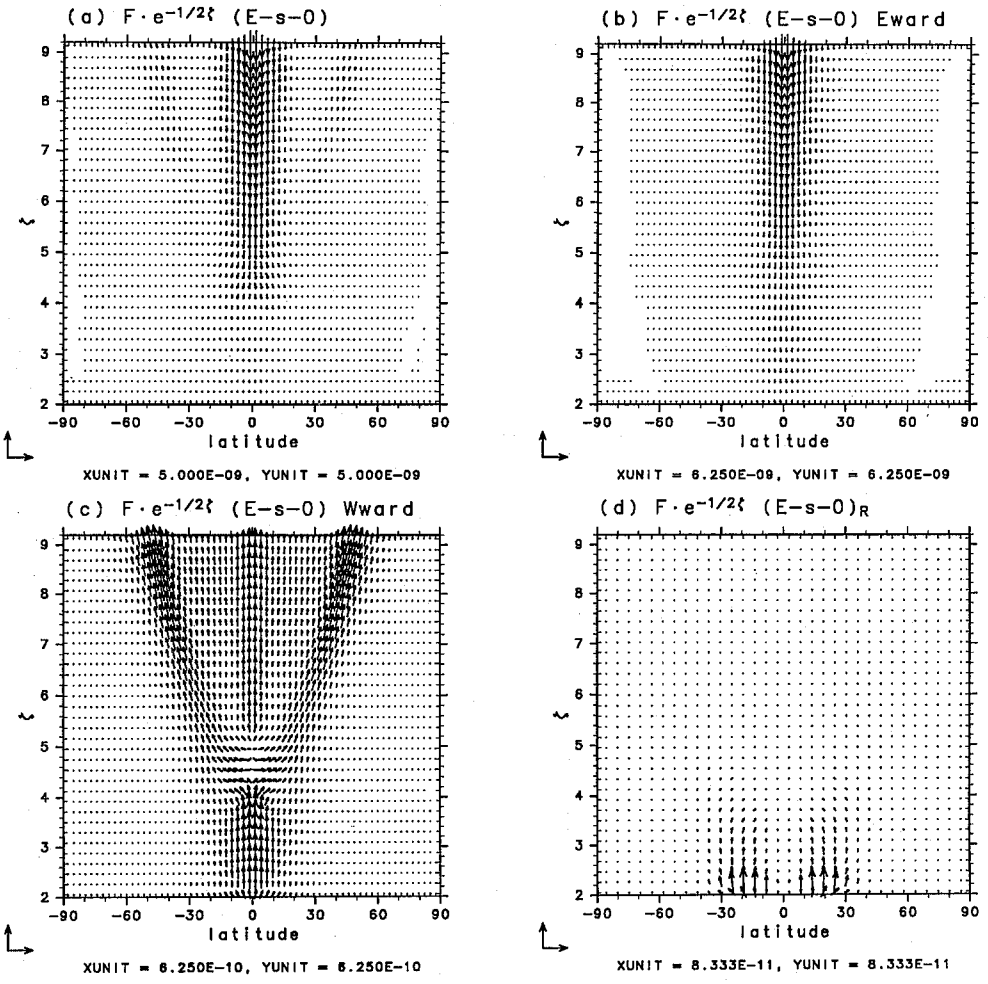

Fig. 8. As in Fig. 7, but for the experiments (E-s-0) and $(\text{E-s-0})_R$.

Unlike the westward-moving waves in early stages as shown in Fig. 2, westward-moving gravity waves which reach the QBO region after $t = 3$ days have phase velocities as slow as -30 ms^{-1}, which is slower than the maximum easterly wind of the QBO (-38 ms^{-1}). Thus there are critical levels for such waves. However, the behavior of such waves is different from the conventional "critical layer absorption"; most of them propagate north- and southward to avoid the critical part in the zonal wind instead of being absorbed there. Similar results are also obtained for the experiments with $\varphi_0 = 10°$.

The time-averaged EP flux obtained in the "l" experiments is trapped near the equator ($|\varphi| \lesssim 20°$) both for the experiments with W and E (Only the results for (W-l-0) are shown in Fig. 9). The eastward momentum is mainly carried by Kelvin waves, while most of the westward one is carried by Rossby waves (and Rossby-gravity waves in the experiments with $\varphi_0 = 10°$). The EP flux in the "l" experiments attenuates in lower altitudes than that in the "s" experiments since waves in the former, on an average, have smaller vertical group velocities.

4.2 EP flux divergence and its effect on the basic states

The time-averaged EP flux obtained in each experiment is multiplied by a factor to get the flux that would be obtained in an experiment in which the stochastic random heating process described in Subsection *2.5* is forced. The converted EP flux is referred to as $\boldsymbol{F}$ in the following. In this subsection, we pay much attention to the divergence of $\boldsymbol{F}$ (div$\boldsymbol{F}$) in the QBO region and in the mesosphere.

Figure 10 shows div$\boldsymbol{F}$ for the experiments with W. It is positive, which means eastward acceleration of zonal mean zonal wind, in the most part around the equator. The acceleration is 0.3 ms^{-1}day^{-1} for the two experiments with $\varphi_0 = 0°$ (a,b). This value is comparable to the observed westerly acceleration of the QBO. The acceleration in the experiments with $\varphi_0 = 10°$ is 0.1–0.2 ms^{-1}day^{-1}.

Although all the experiments of the basic state W produced comparable value of div$\boldsymbol{F}$ to the ob-

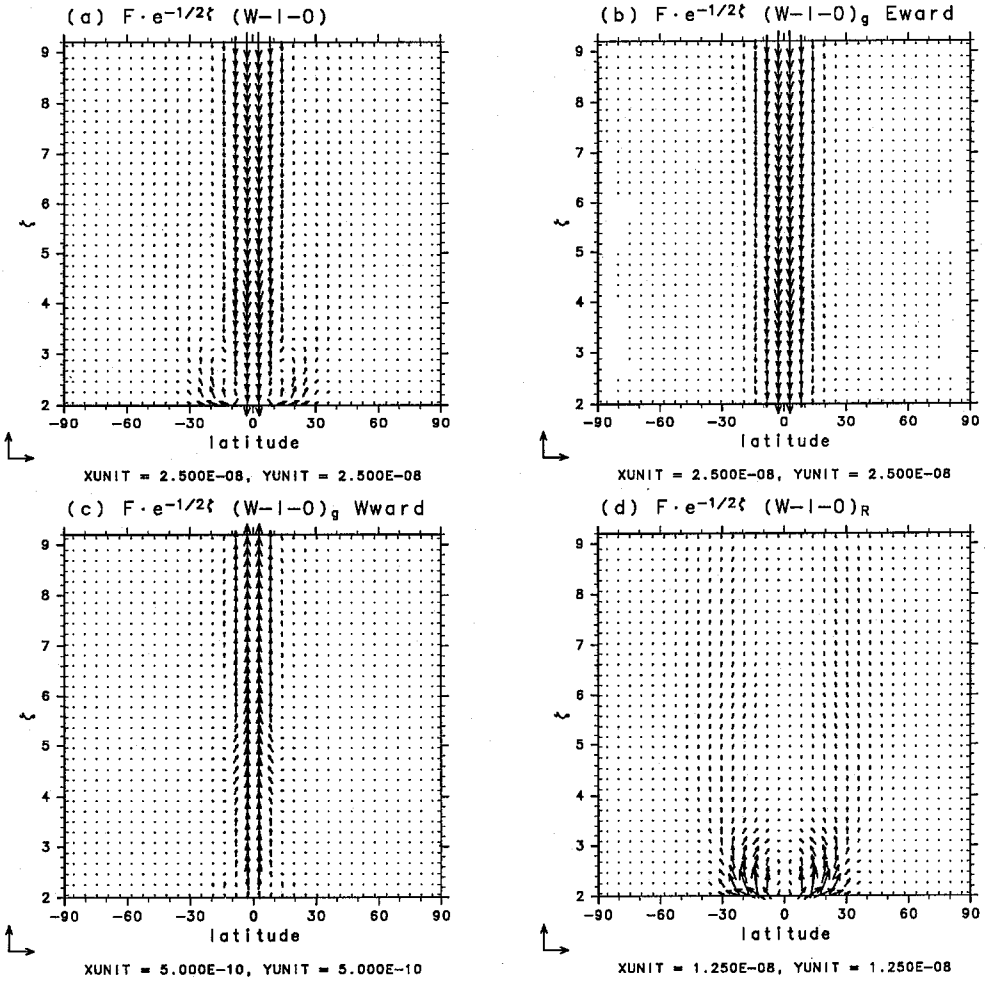

Fig. 9. As in Fig. 7, but for the experiments related to (W-l-0): (a) all components for (W-l-0), (b) eastward-moving components for $(\text{W-l-0})_g$, (c) westward-moving components for $(\text{W-l-0})_g$, and (d) all components for $(\text{W-l-0})_R$.

served westerly acceleration of the QBO, the carriers of the EP flux differ with the experiments. Figure 11 shows the latitudinally-averaged EP flux divergence divided into three zonal wavenumber ranges (s = 1-3, s = 4-7, $s \geq 8$) for the experiments with $\varphi_0 = 0°$. In Experiment (W-s-0), gravity waves of $s \geq 4$ contribute mainly to div$\boldsymbol{F}$, while in Experiment (W-l-0), Kelvin waves of s = 1-3 contribute mainly to it; the predominance of these waves is also confirmed in the experiments with $\varphi_0 = 10°$.

Figure 12 shows div$\boldsymbol{F}$ for the experiments with E. In the easterly shear phase of the QBO, the easterly acceleration is about 0.2–0.3 $\text{ms}^{-1}\text{day}^{-1}$ for the "s" experiments. However, the region of easterly acceleration is limited in height, and there is a region of strong westerly acceleration above the maximum of the easterly wind around $\zeta = 4.5$. Thus the distribution of div$\boldsymbol{F}$ serves to pull the QBO phase downward. Note the westerly acceleration in this region in the experiments with W instead of the effect of pulling the QBO phase downward. This is because the westerly wind in W is small; if it were larger, the maximum of div$\boldsymbol{F}$ would exist in lower altitudes and it would pull the QBO phase downward.

Among the experiments with E, only those with "s" heating events showed comparable value to the observed easterly acceleration of the QBO (Figs. 12a and 12c). This acceleration is due to inertio-gravity waves of large wavenumbers; the contribution of the waves of $s \geq 8$ is dominant as shown in Fig. 11b. On the other hand, the experiments with the "l" heating do not show large easterly acceleration (Figs. 12b and 12d). Actually, there is no easterly acceleration above the equator in Experiment (E-l-0). Easterly acceleration in Experiment (E-l-10) is provided by Rossby-gravity waves of s = 4-7, although it is weak for the QBO acceleration.

The results mentioned above are summarized in Table 2.

In the "s" experiments, westward-moving grav-

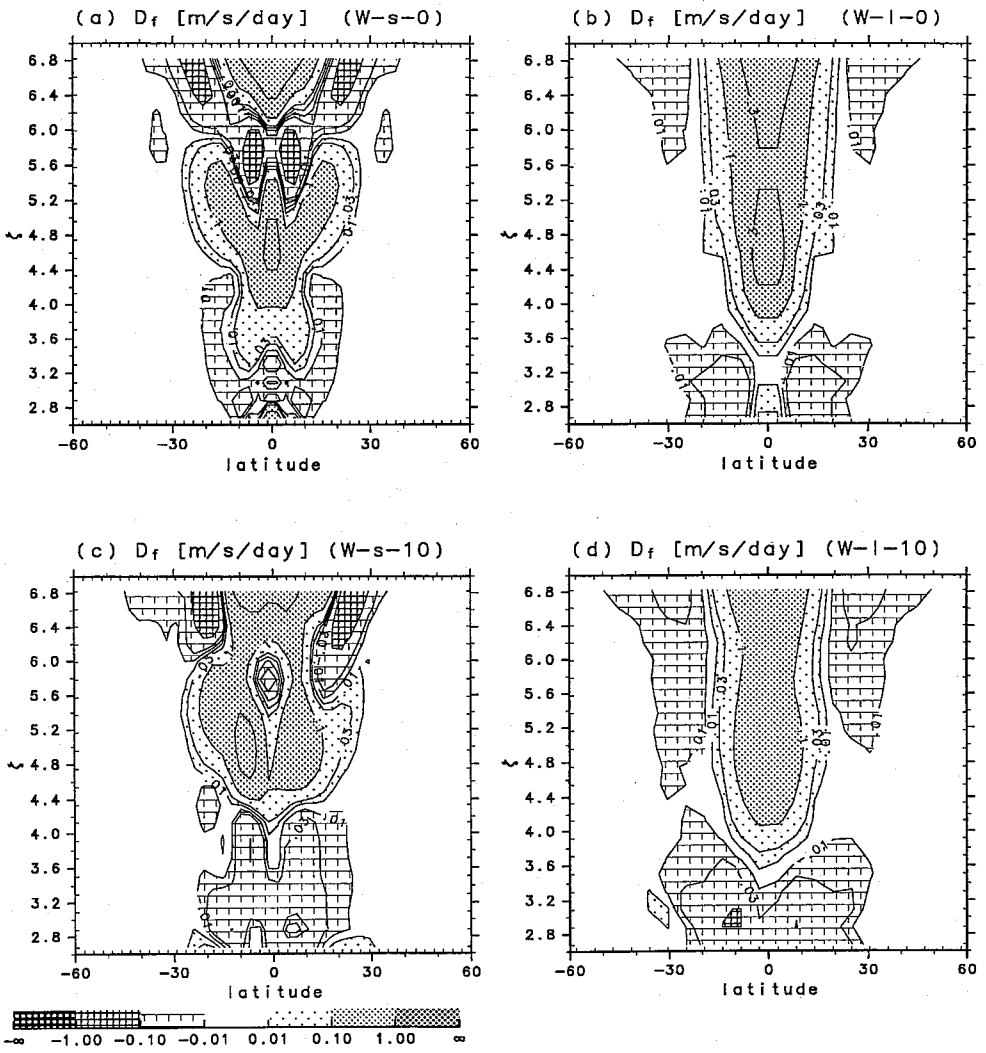

Fig. 10. Meridional section of div$\boldsymbol{F}$ in the experiments with W. Note that div$\boldsymbol{F}$ is the EP flux divergence converted into the quantity that would be obtained by the random heating processes described in Subsection *2.5*.

ity waves, of which the critical latitudes are higher than those of eastward-moving ones in general (Subsection *3.1*), propagate into the mid-latitude mesosphere as shown in Figs. 7 and 8. They are attenuated in the mesosphere and decelerate the westerly wind with div$\boldsymbol{F}$ of from -10 to -3 ms^{-1}day^{-1}. On the other hand, eastward-moving gravity waves in the "s" experiments propagate upward to the equatorial mesosphere, where div$\boldsymbol{F}$ is more than 10 ms^{-1}day^{-1}. Effects of the QBO on the mesosphere by means of these gravity waves are discussed in Section 6.

5. Global normal modes

Figure 13 shows time-longitude sections of geopotential height deviation from the zonal mean at latitude 47° and $\zeta = 6.8$ ($p \sim 1$ hPa) for the three experiments of "l" and $\varphi_0 = 0°$. In each panel, the westward-moving wave of $s = 1$ with a period of 5 days is dominant. This is the global normal mode "5-day wave". In the basic states R (a) and W (b) the 5-day wave has similar amplitude, while in the case of E (c) the amplitude is much larger than that in the other two cases.

Unlike the vertically-propagating waves described in the previous two sections, global normal modes are neutral waves which satisfy the free-slip boundary condition at the surface. Thus the lower boundary condition of the present log-pressure model is not very appropriate to study the normal modes. Therefore we conducted additional experiments with a σ-coordinate model in which the diabatic heating is explicitly forced in the tropical troposphere (see Subsection *2.2*). The initial state is taken from COSPAR International Reference Atmosphere (1986), and two different phases of an idealized QBO are superposed on the basic state.

Simulations with the σ-coordinate model provide

W	"small"	"large"
φ_0=0°	$\sim +0.3$ (Kelvin,IG, $s \geq 4$)	$\sim +0.3$ (Kelvin, $s \leq 3$)
φ_0=10°	$\sim +0.1$ (Kelvin,IG, $s \geq 4$)	$\sim +0.2$ (Kelvin, $s \leq 3$)

E	"small"	"large"
φ_0=0°	~ -0.3 (IG, $s \geq 8$)	> 0
φ_0=10°	~ -0.2 (IG, $s \geq 8$)	~ -0.05 (RG, $4 \leq s \leq 7$)

Table 2. Acceleration of zonal mean zonal wind (div$\boldsymbol{F}$) in the QBO region [ms^{-1}day^{-1}]. Dominant waves for the acceleration are denoted in parentheses: "IG" is inertio-gravity waves and "RG" Rossby-gravity waves. Left: westerly shear phase of the QBO and right: easterly shear.

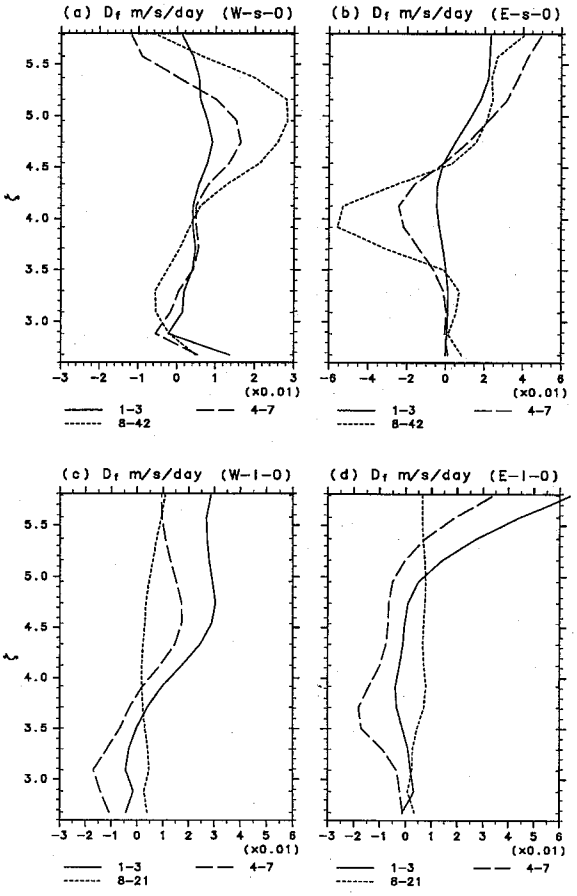

Fig. 11. Meridionally-averaged div$\boldsymbol{F}$ for the experiments with $\varphi_0 = 0$. They are divided into three zonal wavenumber ranges: $1 \leq s \leq 3$ (solid line), $4 \leq s \leq 7$ (dashed line), $8 \leq s \leq 21$ (dotted line).

similar results on the excitation of the global normal modes, that is, the amplitude of the 5-day wave in E is much larger than in W and R, while that in the latter two is comparable.

Since the two numerical models provided similar results, we can conclude that the sensitivity of the global normal modes to the basic state is well described even by the present log-pressure model. The similar results are also obtained for the heating $\varphi_0 = 10°$ with the two models. Global normal modes are also excited in the experiments with the "s" heating. In E, the 5-day wave is also dominant in the geopotential height deviation in high latitudes after $t = 5$ days (not shown); the amplitude is about 1 m. In W, global normal modes are also dominant after $t = 5$ days. However the amplitude of the 5-day wave is larger in E than that in W.

The amplification of the 5-day wave in E occurs during the propagation in the middle atmosphere since the troposphere is excluded in the calculations with the log-pressure model. However, the difference in the basic states between W and E is confined in the equatorial QBO region. In order to elucidate the difference in wave propagation in the two basic states, the EP flux is calculated for the westward-moving component of $s = 1$ with a period of 5 days (Fig. 14). This component is emitted into the stratosphere through low latitudes in both cases. However, it is directed more pole-ward in the QBO region in E (b). This difference in the propagating direction seems to magnify the 5-day wave in E since the wave has large amplitude in mid and high latitudes.

6. Discussion

Among the experiments with the basic state E in the QBO region, the "l" experiments could not reproduce the easterly acceleration comparable to the observed value of the QBO as described in Subsection *4.2*. This implies that random heating processes which consist only of "l" heating events cannot produce the QBO. On the other hand, random heating processes which consist of "s" events may reproduce the QBO. In this case zonal mean zonal wind is accelerated mainly by the gravity waves whose horizontal scales are much smaller than the waves used in the Holton and Lindzen (1972) theory. This is consistent with the estimation that the EP flux of observed Rossby-gravity waves is much smaller than that needed for the downward propagation of the easterly shear of the QBO (Lindzen and Tsay, 1975; Takahashi and Boville, 1992), and that observed Kelvin waves are not sufficient for the downward propagation of the westerly shear of the QBO (Takahashi and Boville, 1992). However, the result that the large-scale heating events are not effective

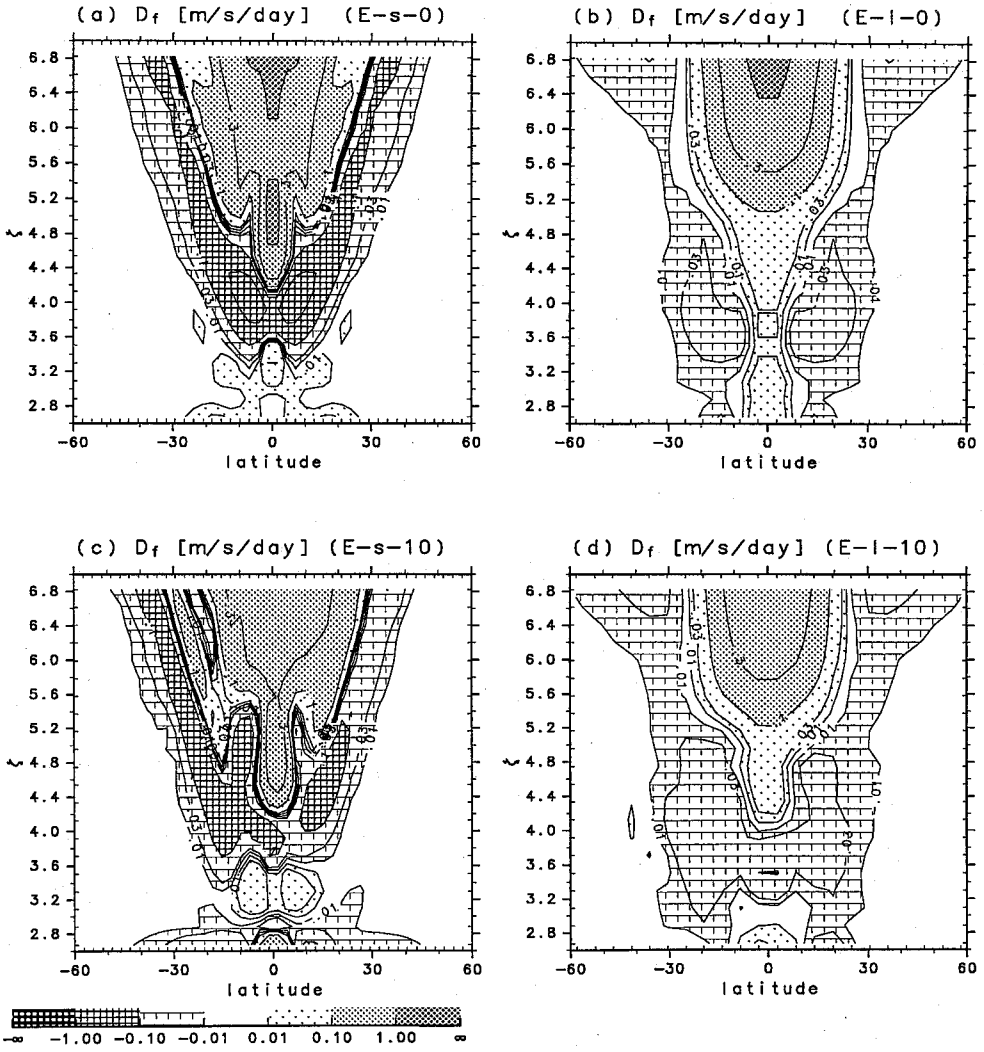

Fig. 12. As in Fig. 10, but for the experiments with E.

to drive the observed QBO may simply be because the heating in this study is idealized artificially, or because no lateral forcing mechanism due to mid-latitude disturbances is considered.

As shown in Section 3, gravity-wave propagation into the mid-latitude mesosphere is affected by the QBO (Figs. 7c and 8c). Westward-moving gravity waves in E propagate into higher latitudes than those in W. As a result, there are large differences in div$\boldsymbol{F}$ in high altitudes between the two basic states as shown in Fig. 15. Note, however, that div$\boldsymbol{F}$ above $\zeta > 10$ may be artificially enhanced due to large Rayleigh friction. The difference in the acceleration of zonal mean zonal wind between the two basic states is about 1–10 $\mathrm{ms}^{-1}\mathrm{day}^{-1}$. In low latitudes, westerly acceleration is larger in E than in W, while it is larger in W in mid-latitudes in the mesosphere. Recently, Burrage *et al.* (1997) found with a measurement by the Upper Atmosphere Research Satellite that the mesospheric zonal wind within a wide band of $|\varphi| \lesssim 30°$ varies out of phase with the stratospheric QBO. Namboothiri *et al.* (1997) also found with archives of the MU radar (136°E, 35°N) data that the mid-latitude mesospheric zonal wind has variations which seem to be coupled with the equatorial stratospheric QBO. These observations may be explained by the QBO modulation of the propagation of gravity waves excited thermally in the tropical troposphere.

The result obtained in Section 5 that the amplitude of the global normal mode 5-day wave suffers strong QBO modulation is robust if the wave is excited in the tropics, since both of the numerical models provided this result for a wide variety of the parameters of the heating. Since this modulation occurs through the wave propagation in the QBO region, it is not peculiar to the localized heating we assumed but is a general consequence when the source of the wave is located in the tropics. However, such a modulation has not been reported for the real atmosphere. Hirooka and Hirota (1989) studied long-term variability of the normal mode Rossby waves,

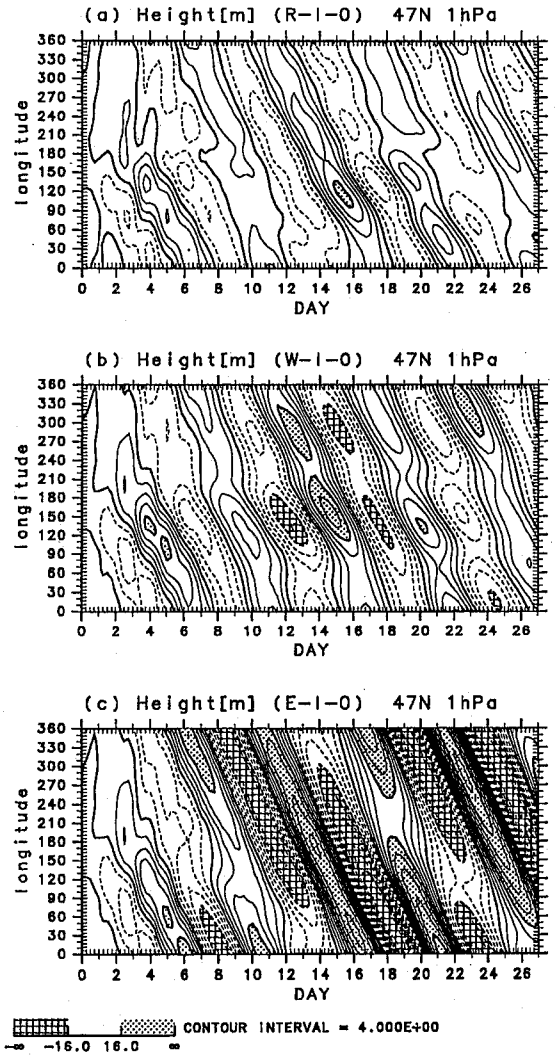

Fig. 13. Time-longitude sections of the deviation of geopotential height from the zonal mean at $\varphi = 47°$ and $\zeta = 6.8$ ($p \sim 1$ hPa) for the experiments (R-l-0), (W-l-0) and (E-l-0).

and showed a "calendar" of the appearance of the modes (their Fig. 6), in which we can not observe a clear time variation of the appearance coupled with the QBO. Thus our numerical results suggest that the source of the observed 5-day wave is not or not only in the tropics, but a considerable portion of the wave is excited in mid or high latitudes. However, a further observational study will be required to verify this suggestion. Note the recent study by Cheong and Kimura (1995) that suggests observationally and numerically that the 5-day wave in the real atmosphere is excited mainly in the antarctic region.

7. Conclusions

Propagation of waves excited by localized episodic heating in the tropics and their effect on the middle atmosphere are investigated numerically with a global primitive-equation model. A realistic radiation scheme for the middle atmosphere is incorporated in the model. Equinoctial initial (basic) states with two opposite QBO phases W (the westerly shear phase) and E (the easterly shear phase) and a resting one R are used to calculate their responses to the heating with various combinations of its parameters. The key parameters are the horizontal and time scales of the heating: we used two combinations of them named "s" (small: $\Lambda = 3°$, $\Phi = 3°$, $T = 0.1$ days) and "l" (large: $\Lambda = 10°$, $\Phi = 10°$, $T = 0.5$ days).

Time evolutions of the response of the three basic states are similar to those obtained in the linear model by Horinouchi and Yoden (1996); there are two characteristic patterns depending on the time scale of the heating. For the "s" heating whose duration is smaller than a day, gravity wave response expands concentrically at the beginning and then the response spreads zonally in low latitudes. For the "l" heating whose duration is larger than a day, on the other hand, the "Gill pattern" appears at the beginning and then the response spreads zonally in low latitudes too. In the "s" experiments, the time-averaged EP flux over the integration period of 30 days consists mainly of gravity waves including Kelvin waves in the middle atmosphere. In the "l" experiments, on the other hand, it consists mainly of Kelvin waves, Rossby waves and Rossby-gravity waves. Waves in the former experiments in general hold their wave activity to higher altitudes than the latter because of larger vertical group velocities.

Gravity waves in the "s" experiments propagate to the mesosphere. In equinoctial conditions, the westward-moving gravity waves (waves of westward phase propagation) propagate to the mid- and high-latitude mesosphere, while the eastward-moving ones propagate to the equatorial mesosphere. This is because the westward-moving waves have higher critical latitudes than the eastward-moving ones owing to the westerly wind in mid-latitudes. The QBO in the equatorial lower stratosphere also affects the wave propagation in meridional planes. The strong easterly wind in the easterly shear phase of the QBO prevents the upward propagation of the westward-moving gravity waves, and a considerable portion of them propagates north- and south-ward to avoid the critical layer absorption. Above the QBO region, eastward- (westward-) moving waves in E have larger (smaller) amplitude than in W, while this relationship is reversed in the QBO region; both are explained by the WKB theory.

As summarized in Table 2, all the experiments with W reproduced the westerly acceleration of the mean zonal wind comparable to or a little smaller than the observational value in the westerly shear phase of the QBO. In the "s" experiments, gravity waves of zonal wavenumber s larger than 3 carry

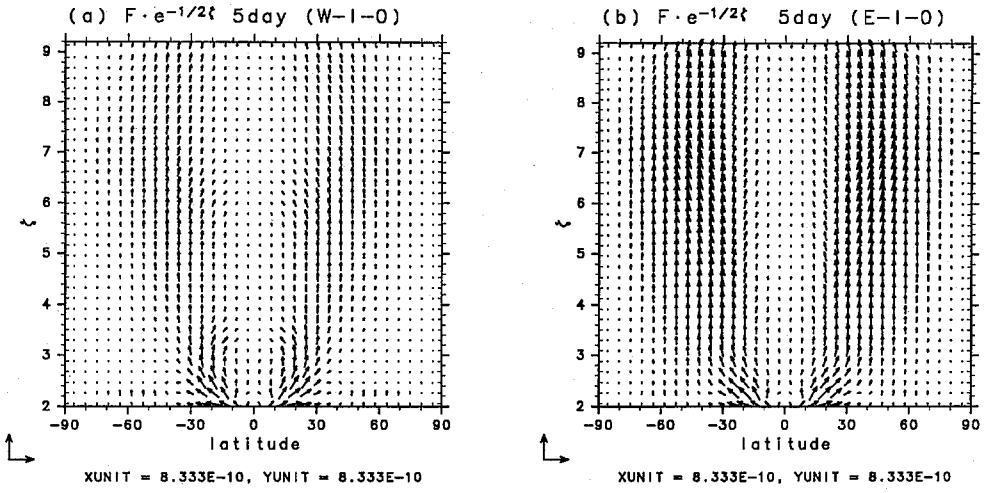

Fig. 14. Time-averaged EP flux of the westward-moving disturbances of $s = 1$ with a period of 5 days for the experiments (W-l-0) and (E-l-0).

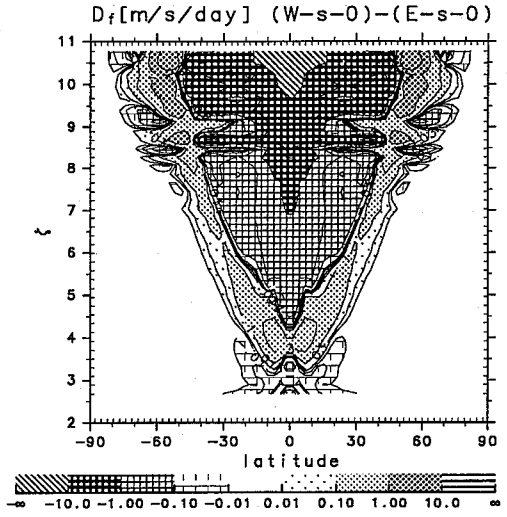

Fig. 15. Difference in div$\boldsymbol{F}$ between the two experiments (W-s-0) and (E-s-0).

most of zonal momentum, while in the "l" experiments Kelvin waves of s = 1-3 carry most of it. On the other hand, among the experiments with E, only the "s" experiments could reproduce the easterly acceleration comparable to the observation in the easterly shear phase of the QBO. Thus random heating processes which consist only of "l" heating events cannot produce the QBO, while those consist of "s" heating events may produce it.

EP flux and its divergence of the gravity waves incident on the low- and mid-latitude mesosphere are affected by the QBO. This may explain the recent observations of quasi-biennial variations in the low and mid-latitude mesosphere.

The global normal mode 5-day wave suffers a strong QBO modulation if its source is located in the tropics; it has larger amplitude in the easterly shear phase than in the westerly one. However, such a QBO modulation is not observed in the real atmosphere. Thus it is expected that the source of the observed 5-day wave is not or not only in the tropics, but a considerable portion of the wave must be excited in mid or high latitudes.

Acknowledgments

GFD-DENNOU Library was used for drawing figures. The numerical models used in this study are based on the AGCM5 code in this library. Numerical calculation was done on the KDK system at RASC, Kyoto University. This work was supported in part by the Grant-in-Aid for the Cooperative Research with Center for Climate System Research, University of Tokyo.

References

Bergman, J.W. and M.L. Salby, 1994: Equatorial wave activity derived from fluctuations in observed convection. *J. Atmos. Sci.*, **51**, 3791–3806.

Burrage, M.D., R.A. Vincent, H.G. Mayr, W.R. Skinner, N.F. Arnold and P.B. Hays, 1997: Long-term variability in the equatorial mesosphere and lower thermosphere zonal winds. *J. Geophys. Res.*, in press.

Cheong, H.-B. and R. Kimura, 1995: Excitation of the 5-day Wave. *Proc. Japan Acad.*, **71**, Ser. B, No. 4, 115–120.

COSPER International Reference Atmosphere, CIRA, 1986, Pergamon Press, Oxford OX3 0BW, England.

Garcia, R.R. and M.L. Salby, 1987: Transient response to localized episodic heating in the tropics. Part II: Far field behavior. *J. Atmos. Sci.*, **44**, 499–530.

Gill, A.E., 1980: Some simple solutions for heat-induced tropical circulation. *Quart. J. Roy. Meteor. Soc.*, **106**,447–462.

Hayashi, Y., 1976: Non-singular resonance of equatorial waves under the radiation condition. *J. Atmos. Sci.*, **33**, 183–201.

Hirooka, T. and I. Hirota, 1989: Further evidences of normal mode Rossby waves. *Pure Appl. Geophys.*, **130**, 277–289.

Holton, J.R., 1972: Waves in the equatorial stratosphere generated by tropospheric heat sources. *J. Atmos. Sci.*, **29**, 368–375.

Holton, J.R. and R.S. Lindzen, 1972: An updated theory for the quasi-biennial cycle of the tropical stratosphere. *J. Atmos. Sci.*, **29**, 1076–1080.

Horinouchi, T. and S. Yoden, 1996: Wave excitation by localized heating in the tropics and its propagation into the middle atmosphere. *J. Meteor. Soc. Japan*, **74**, 189–210.

Itoh, H., 1977: The response of equatorial waves to thermal forcing. *J. Meteor. Soc. Japan*, **55**, 222–239.

Johnson, R.H., 1992: Heat and moisture sources and sinks of Asian monsoon precipitating systems. *J. Meteor. Soc. Japan*, **70**, 353–372.

Lindzen, R.S., 1971: Equatorial planetary waves in shear: Part I. *J. Atmos. Sci.*, **28**, 609–622.

Lindzen, R.S. and C.-Y. Tsay, 1975: Wave structure of the tropical stratosphere over the Marshall islands area during 1 April–1 July 1958. *J. Atmos. Sci.*, **32**, 2008–2021.

Manzini, E. and K. Hamilton, 1993: Middle atmospheric traveling waves forced by latent and convective heating. *J. Atmos. Sci.*, **50**, 2180–2200.

Mellor, G.L. and T. Yamada, 1974: A hierarchy of turbulence closure models for planetary boundary layers. *J. Atmos. Sci.*, **31**, 1791–1806.

Namboothiri, S.P., T. Tsuda and T. Nakamura, 1997: Interannual variability of mesospheric mean winds observed with the MU radar. *Taikiken Shinpojumu*, **10**, in press.

Salby, M.L. and R.R. Garcia, 1987: Transient response to localized episodic heating in the tropics. Part I: Excitation and short-time near field behavior. *J. Atmos. Sci.*, **44**, 458–498.

Takahashi, M. and B.A. Boville, 1992: A three-dimensional simulation of the equatorial quasi-biennial oscillation. *J. Atmos. Sci.*, **49**, 1020–1035.

U.S. Standard Atmosphere, 1976, NOAA-S/T76-1562, Supt. of Documents, U.S. Govt. Printing Office, Washington, D.C.

Zhu, X., 1994: An accurate and efficient radiation algorithm for middle atmosphere models. *J. Atmos. Sci.*, **51**, 3593–3614.

熱帯に局在した非定常な加熱により励起される波動の中層大気への伝播と作用：QBOの2局面間の比較

堀之内武・余田成男

（京都大学大学院理学研究科 地球惑星科学専攻 地球物理学教室）

熱帯対流圏に局在した非定常な加熱により励起される波動の中層大気への伝播と作用を全球プリミティブ方程式モデルを用いて数値的に調べた。このモデルは中層大気のための精度のよい放射スキームを積んでいる。春・秋分の場に異なる準2年周期振動(QBO)の位相を重ねた2つの初期場を用いて伝播と作用を比較した。

春・秋分の初期場の応答の時間発展は Horinouchi and Yoden (1996) が得た静止大気の線形応答の時間発展と似ている。加熱の持続時間が短ければ(1日以下程度)中層大気におけるエリアッセン-パルム(EP)フラックスはケルビン波を含む重力波により主にもたらされる。一方, 持続時間が長ければ(1日以上程度)ケルビン波, ロスビー波、ロスビー重力波の貢献が主となる。

QBOの西風シアー期では、広い範囲の加熱のパラメター値に関して現実的かやや弱い程度のQBO域の西風加速が得られる。一方、東風シアー期では加熱のスケールが大きいと(約1日以上、数千km)現実的な大きさの東風加速は得られない。低・中緯度の中間圏に伝播する重力波はQBOの影響を受ける。これに伴う重力波によるEPフラックス収束の変動が観測される低・中緯度中間圏のQBO的変動をもたらしているかも知れない。

全球ノーマルモード「5日波」はQBOの位相に敏感である。しかし現実大気中にはそのようなQBO依存性が観測されていないので、5日波の励起源は熱帯にばかりにあるということはなく、少なからぬ量が中高緯度で励起されていると考えられる。